

High visible-light photocatalytic performance of natural hematite ore composited with ZnO nanomaterials

Xin X. Yu¹, Fang Z. Dong¹, Bao Dong¹, Liang Liu¹, Yan Wu^{1,2*}

¹Faculty of Materials Science and Chemistry, China University of Geosciences (Wuhan), Wuhan, 430074, P. R. China

²Engineering Research Center of Nano-Geo Materials of Ministry of Education China University of Geosciences, Wuhan, 430074, China

*Corresponding author: Tel: +86 27 67883736; E-mail: wuyan@cug.edu.cn

Received: 10 September 2016, Revised: 18 November 2016 and Accepted: 21 November 2016

DOI: 10.5185/amlett.2017.7079

www.vbripress.com/aml

Abstract

Natural hematite ore is used as a novel material for visible photocatalyst. The hematite was composited with needle-shaped ZnO via a hydrothermal approach. This hematite-based system exhibits excellent photodegradation for rhodamine (RhB) within 30 min when the hematite is hybridized with wurtzite-structured ZnO under visible light irradiation. The formation of a hybrid hetero-junction was shown by transmission electron microscope. The photocatalytic activity of the hetero-junction was evaluated by the photodegradation of RhB dye. The high photocatalytic activity observed under visible light is discussed on basis of the coupling of the hybrid hetero-junction band structure. Copyright © 2017 VBRI Press.

Keywords: Natural hematite, needle-shaped ZnO, hybrid hetero-structure, photocatalyst.

Introduction

In recent years, nanocomposite semiconductors have been largely investigated because of their important applications in environment and energy fields [1-3]. Their multifunctional properties can be expressed in terms of their size, composite, and structural orders. However, the high-cost of synthesized materials in current photocatalysts and greater recognition of the need for environmental protection have driven efforts to find ecologically friendly, natural minerals for use in low-cost photocatalyst. α -Fe₂O₃ (hematite) is a semiconductor with a band gap of 1.9-2.2 eV. It possesses of a wide absorption in the solar light spectra [4, 5]. The natural hematite is an abundant and inexpensive mineral, of which the current market price is about 80 dollars per ton and its current world reservation is more than 370 billion tons. It has recently been studied as a promising oxygen carrier and electrolyte material for water splitting and fuel cells [6-8]. Some wide band gap metal oxide semiconductors, e.g. TiO₂, ZnO and WO₃ have attracted increasing attention due to its steady photocatalytic properties, non-toxic, highly photoactive and good ultraviolet (UV) light absorption [9, 10]. But its band gap is wide (such as ZnO was 3.37 eV) with a absorption peak lower than 400 nm, it can only absorb a small fraction of the whole solar spectra [11, 12]. Thus, a critical challenge is faced due to low efficiency and high manufacture cost. The new trend is to develop narrow band gap semiconductors in two strategies. One is to employ doped or hybridized technologies to widen the absorbing spectra

[13]; The other is to develop various new narrow bandgap materials [14, 15].

Recently iron oxides exhibit high photocatalytic performances as a promising candidate for development of visible light photocatalyst due to its adequate absorption of visible light up to 560 nm [8, 16], very positive valence band energy, and good stability. To develop next-generation visible light photocatalyst, we focus on economically viable iron ore materials. Hereby we develop a radically new and simple natural ore composited with ZnO nanomaterials that exhibits both high photodegradation of organic molecules and good recycling properties. The natural hematite-ZnO composites were fabricated and investigated as visible light photocatalysts.

Experimental

Material

Materials: All the reagents were analytical grade, and the raw hematite powder was originated from Laiwu (LW) zone of Shandong province of China.

Synthesis of ZnO and LW-ZnO composite

ZnO nanomaterials: 15 mL of sodium hydroxide (4.0 mol·L⁻¹) was added drop-wise into 20 mL of zinc acetate dehydrate (Zn(CH₃COO)₂·2H₂O) (1 mol·L⁻¹) with vigorous stirring, until drops out and keeping stirring for 15 min to obtain the homogeneous solution. This solution was placed into a three-necked flask, while it was heating

and refluxed at 105 °C for 3 h. After the solution cooled to room temperature, the wet product was filtrated and dried in a vacuum oven at 70 °C for about 10 h. More details could be referred to the earlier report [4].

Natural hematite with ZnO composite: different weight ratio of as-obtained ZnO nanopowders and raw hematite ore (5%, 10%, 15%, and 20%) were put into a 50 ml breaker then mixed 4 ml double-distilled water, ultrasonicated for about 20 min. Sequentially, transfer the mixed liquor to a Teflon reactor at 120 °C for 12 h. The as-precipitation was washed and then heated in an oven at 70 °C for 5 h, for use. The samples are labeled respectively as 5% ZnO-LW, 10% ZnO-LW, 15% ZnO-LW, and 20% ZnO-LW.

Characterization of samples

The phase structure was analyzed using a D8-FOCUS X-ray diffractometer. Transmission electron microscope (TEM) images were obtained by a CM12/STEM transmission electron microscopy with an accelerating voltage of 120 V. The Brunauer-Emmett-Teller (BET) surface area of the samples were measured at liquid nitrogen temperature (77.4 K) using a nitrogen adsorption apparatus (ASAP-2020, Micromeritic, USA). Ultraviolet-visible (UV-vis) spectra of solid powders were performed on a Lambda 35, double beam UV-vis absorption spectrometer equipped with a deuterium lamp and a tungsten-halogen lamp. Room temperature photoluminescence (PL) of the samples were recorded on a FP-6500 fluorescence spectrophotometer with a xenon arc lamp as the excitation source. The evaluation of the photocatalytic properties was referred to our earlier method [7]. The simulated solar light irradiation was provided by a 300 W simulated solar light and a 420 nm light filter was put on the beaker to cut off the UV light below 420 nm. The absorption value of rhodamine (RhB) was taken at the peak absorption upon 554 nm. The magnetic properties of the composites were characterized via a vibrating sample magnetometer (VSM, Model 155 EG&G Princeton Applied Research) with a maximum applied field of ± 1 Tesla.

Results and discussion

Phase structure and morphology

Fig. 1 depicts the X-ray diffraction (XRD) patterns of LW hematite ore, ZnO, and LW hematite-ZnO composite materials and the morphology of 15% ZnO-LW. The main phase structures of raw LW ore are hematite (Fe_2O_3), quartz (SiO_2) and calcite (CaCO_3). There are characteristic peaks of pure ZnO, which are identified as the standard hexagonal ZnO (JCPDS card No. 361451) [17]. The XRD results of the composites show only hematite and ZnO structures, and there are no other new phases occur. The 15% ZnO-LW composite morphology shows large contacts and interfaces between the mineral hematite and ZnO; these contacts and interfaces substantially affect the electron transport properties.

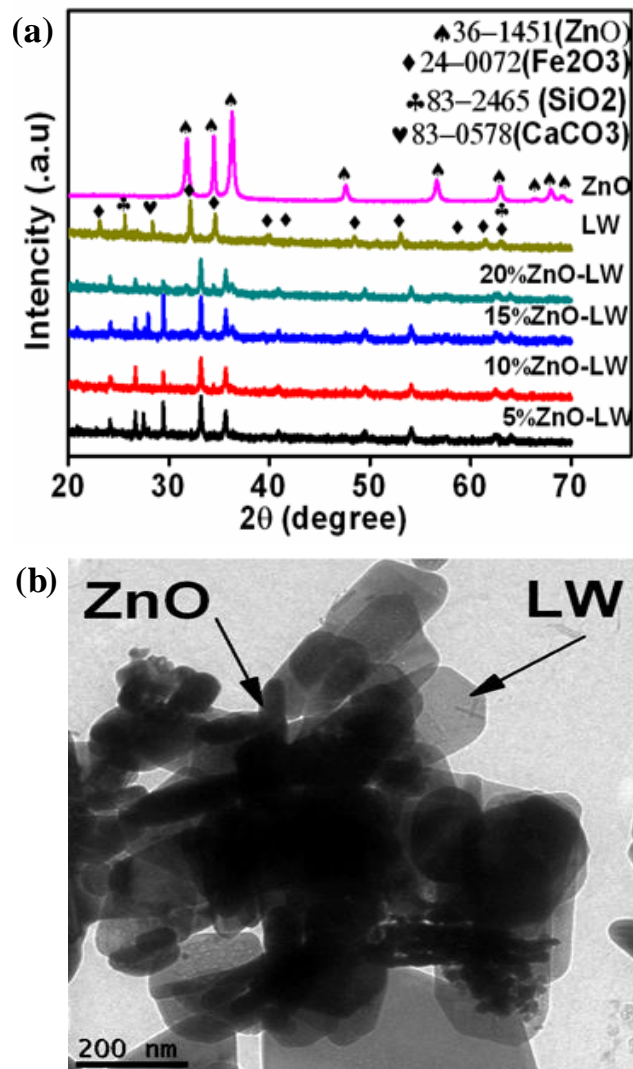


Fig. 1. (a) X-ray diffraction patterns of the raw LW ore, ZnO, and the hematite-ZnO composites. (b) TEM image of 15 % ZnO-LW sample.

Optical and BET analysis

The UV-vis absorption in the wavelength range of 250–850 nm of the prepared samples were investigated and the band gap (E_g , eV) is determined by the equation of $\alpha h\nu = K(h\nu - E_g)^{n/2}$, referring to **Table 1**, where α , h , ν , E_g , and K are absorption coefficient, Plank constant, light frequency, band gap, and a constant, respectively [18].

Table 1. Calculated bandgap of samples ZnO, LW and different mass ratio ZnO composite with LW hematite.

Sample	LW	10%ZnO-LW	15%ZnO-LW	20%ZnO-LW	ZnO
(E_g) (eV)	2.24	2.74	2.99	3.03	3.21

The band gap of ZnO is about 3.21 eV, 10% ZnO-LW is 2.74 eV, 15% ZnO is 2.99 eV and 20% ZnO is 3.03 eV, while the LW hematite is about 2.24 eV, which is consistent with the fabricated hematite [19]. Compared with ZnO, the E_g value of ZnO-LW composite decreases with the higher content of LW, which is consistent with

the bandgap values of $\text{Fe}_2\text{O}_3/\text{ZnO}$ composites [20]. Besides, the E_g value of ZnO-LW composite is slightly increase with the amount of ZnO ratio, which is attribute to the UV absorption of ZnO itself. All these changes play great effect on their photocatalytic activity.

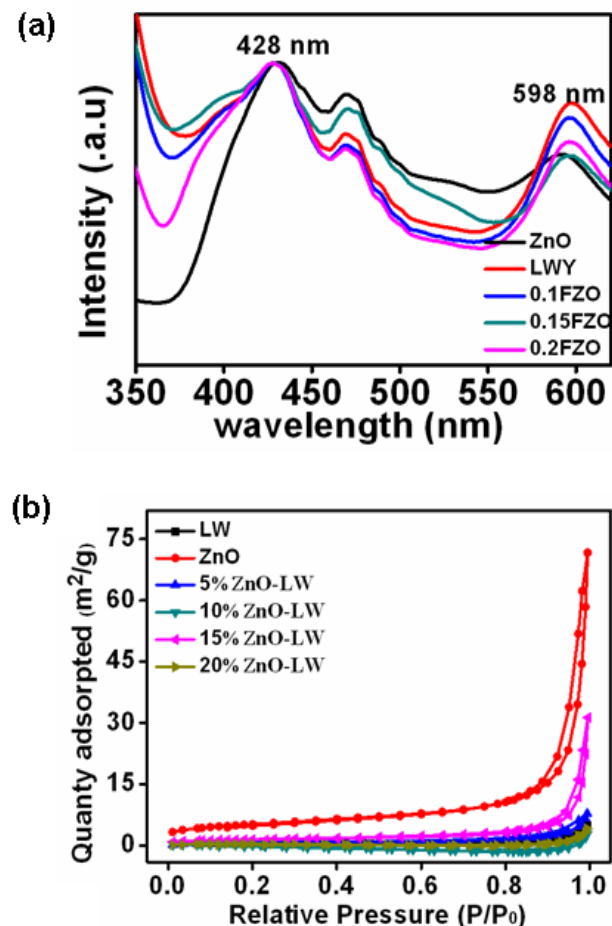


Fig. 2. (a) PL spectra and (b) N_2 adsorption-desorption isotherms of LW, ZnO, and various mass ratios of ZnO-LW composites.

Fig. 2a shows the room temperature PL emission spectra of pure ZnO , hematite, and the samples with different mass ratio ZnO composite to hematite. There are two-type significant emissions: violet emission centered at 428 nm and visible emissions at 460–598 nm, which are attributed to the structural defects, such as oxygen vacancies and hetero-junction structure of the catalysts [21]. The PL intensity of the visible emission band of the pure ZnO sample is weaker than those composite samples. The N_2 adsorption-desorption isotherms of the samples ZnO , LW and various ZnO-LW were conducted at room temperature. The results are shown in Fig. 2b. It can be seen that the adsorption-desorption isotherms may be classified as type IV isotherm which shows a H_2 hysteresis loop of the mesoporous materials [22, 23]. This indicates the samples as typical mesoporous structure materials according to the conventional classification. The mesopores allow light to scatter inside their pore channel, thus enhance the harvesting of the light [24]. The N_2 adsorption capacity of ZnO was higher than other samples, and when ZnO composite with LW, the adsorption capacity was changing. After the composite,

the adsorption capacity of LW increase at first, but when ZnO mass ratio up to 20%, the surface area of the sample decrease.

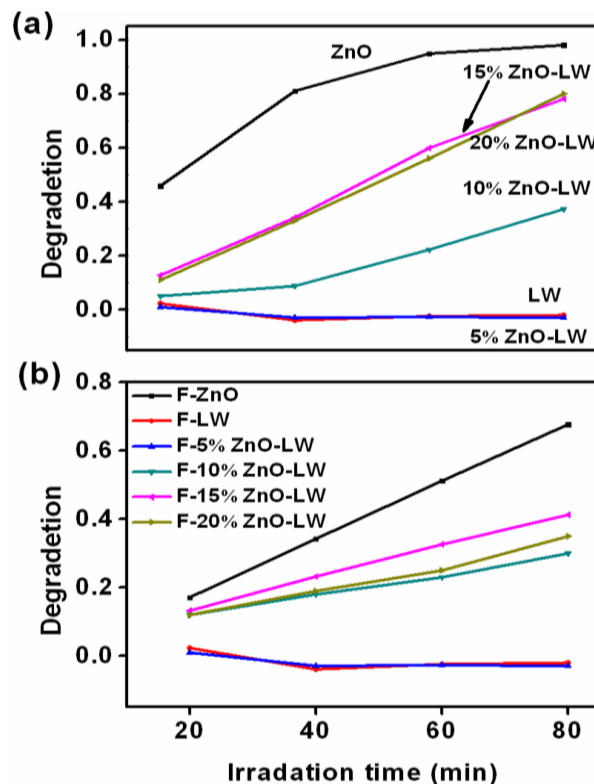


Fig. 3. Photocatalytic activity of RhB solution as a function of irradiation time in the presence of different samples under the solar irradiation (a) without and (b) with a 420 nm visible light filter.

Photocatalytic activity

The photocatalytic performance of the as-prepared samples was evaluated by monitoring the degradation behavior of RhB , as shown in Fig. 3. No dye degradation in solution of RhB can be observed in the absence of the photocatalyst, and at the same conditions from a blank experiment. But in a continual fading of the coloration in RhB solution with reaction time in presence of the samples was observed, implying a steady and continuous degradation of the organic dye. We can see also that the sample ZnO-LW and LW hematite have no adsorption with the RhB molecules. And also there was very low photodegradation of RhB solution in the presence of hematite and 5% ZnO-LW under solar light irradiation in Fig. 3a. By increasing the content of ZnO nanorods up to 15%, the photodegradation rate rapidly increases. However, further increasing the ZnO content, the photodegradation rate tends to slightly decrease. While after using a 420 nm visible light filter, as shown in Fig. 3b, there was also very low photodegradation of RhB solution both in the presence of LW and 5% ZnO-LW . But for the 15% ZnO-LW sample, the photodegradation value only reduces about 11% within 40 min, which indicates that the 15% ZnO-LW sample expand the absorption of visible light up 400 nm. The results prove that in the 15% ZnO-LW sample the formation of hetero-junction structure between ZnO and hematite is formative [25, 26].

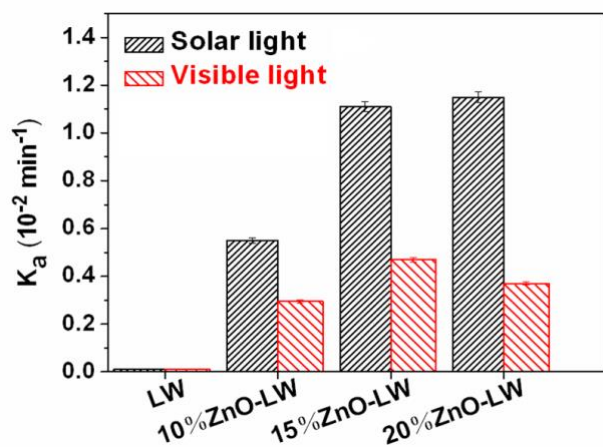


Fig. 4. Degradation kinetics rates K_a of RhB solution in the presence of ZnO-LW catalysts under the solar and visible light irradiation, respectively.

The degradation kinetics rate (K_a) is determined through the Langmuir-Hinshelwood kinetic model. The obtained result from the linear regressions for degradation of RhB is summarized and presented in Fig. 4. For pure natural LW hematite, the photodegradation rate K_a for degradation of RhB is neglectable due to its dominant absorption of dye molecules. It starts to rapidly increase with the content of ZnO nanorods up to 15%, and then slightly decreases with overloading of ZnO.

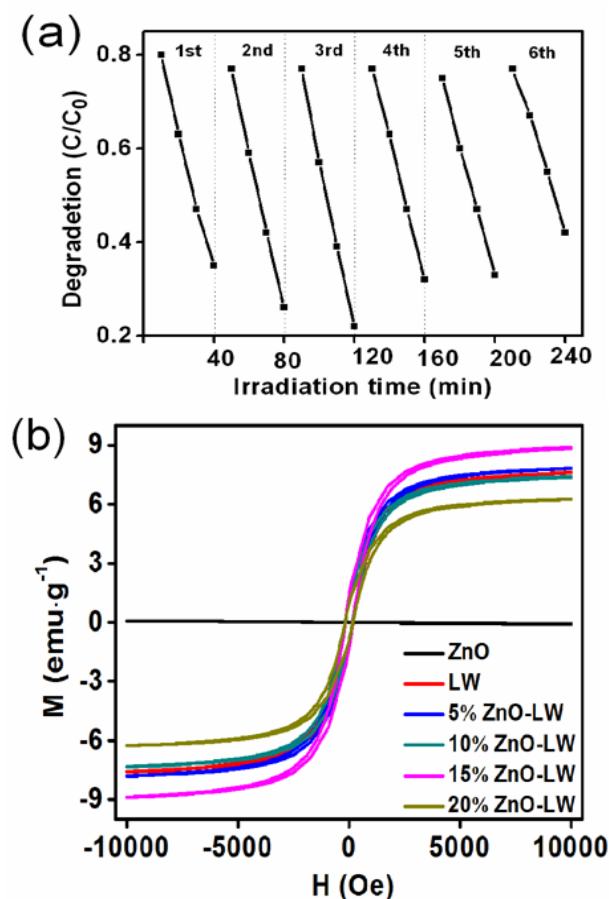


Fig. 5. (a) The stability of 15% ZnO-LW photodegradation of RhB solution and (b) Magnetic hysteresis data of the samples for ZnO-LW catalysts.

Decolorization efficiency of the dye solution, which determines the adsorption of the organic compound on the surface of ZnO-LW and represents an important reaction step in the overall mechanism of dye oxidation. Adsorption and RhB degradation seem to be favored at pH around the zero point charge pH (pH_{zpc}), i.e. around neutral for the ZnO-LW, which is close to the reported pH_{zpc} of 7–8 for Fe_2O_3 nanoparticles [27].

In addition to photocatalytic efficiency, the usability of photocatalyst is also a key issue for practical application. Therefore, recycling tests with repeated use of ZnO-LW hetero-structure photocatalyst in six consecutive reactions were carried out under the same conditions. As shown in Fig. 5a, after six recycles of RhB degradation, the 15% ZnO-LW composite still shows comparatively high photocatalytic activity. Moreover, magnetic property for various ZnO-LW samples is close to that of the LW, shown in Fig. 5b. It exhibits the saturation magnetization values of various ZnO-LW composites are close to the pristine LW sample, which indicates that the hybrid catalysts possess a good magnetic separation for this system.

Conclusion

We have successfully synthesized efficient ZnO nanoparticles with two shapes needle-like and nanosheet shapes. And ZnO/hematite heterogeneous structures have been prepared by hydrothermal method. These samples have been extended the absorption of light from UV light to visible light and enhanced the efficiency of absorbing of solar light. These results can impact on the design and utilize of new photocatalytic hetero-junctions based on semiconductor nanomaterials and morphology. We believe that using of the natural materials with widespread, abundant and cheap resources is a very inexpensive and efficient way to remove the organic dye from water.

Acknowledgements

This work was supported by the National Natural Science Foundation of China (No. 51302252), Chengguan Talented Youth Development Foundation, and the Fundamental Research Funds for National Universities, China University of Geosciences (Wuhan).

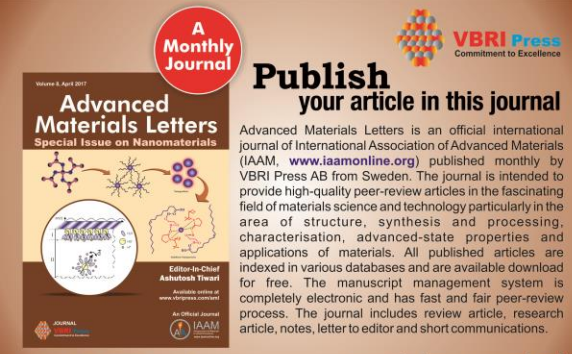
Author's contributions

Conceived the plan: XY, YW; Performed the experiments: XY, ZD, BD, LL; Data analysis: XY, ZD, BD, LL, YW; Wrote the paper: XY, YW.

References

- Tian, J.; Sang, Y. H.; Zhao, Z. H.; Zhou, W. J.; Wang, D. Z.; Kang, X. L.; Liu, H.; Wang, J. Y.; Chen, S. W.; Cai, H. Q.; Huang, H.; *Small*, **2013**, *9*, 3864-3872.
DOI: [10.1002/sml.201202346](https://doi.org/10.1002/sml.201202346)
- Shukla, S.K.; Tiwari, A.; Parashar, G.K.; Mishra, A.P.; Dubey, G.C.; *Talanta*, **2009**, *80*, 2, 565.
DOI: <http://dx.doi.org/10.1016/j.talanta.2009.07.026>
- Wu, Y.; Tamaki, T.; Volotinen, T.; Lova, L. B.; Rao, K. V.; *J. Phys. Chem. Lett.*, **2010**, *1*, 89-92.
DOI: [10.1021/jz900008y](https://doi.org/10.1021/jz900008y)
- Xie, J.; Zhang, L.; Li, M.X.; Hao, Y.J.; Lian, Y.W.; *Ceram. Int.*, **2015**, *41*, 9420.
DOI: [10.1016/j.ceramint.2015.03.320](https://doi.org/10.1016/j.ceramint.2015.03.320)
- Bonamali, P.; Maheshwar, S.; Gyoichi, N.; *Mater. Chem. Phys.*, **1999**, *59*, 254.
DOI: [10.1016/S0254-0584\(99\)00071-1](https://doi.org/10.1016/S0254-0584(99)00071-1)

- 6 Zong, X.D.; Li, W.; Zhao, H.S.; Fang, C.C.; Peng, C.; *Geolo. Res.*, **2011**, 20, 370.
DOI: [10.13686/j.cnki.dzyzy.2011.05.008](https://doi.org/10.13686/j.cnki.dzyzy.2011.05.008)
- 7 Wang, L.Q.; Wu, Y.; Chen, F.Y.; Yang, X.; *Prog. Nat. Sci.*, **2014**, 24, 6.
DOI: [10.1016/j.pnsc.2014.01.002](https://doi.org/10.1016/j.pnsc.2014.01.002)
- 8 Dauth, A.; Love, J.A.; *Dal. Tra.*, **2012**, 41, 7782.
DOI: [10.1039/C2DT30639E](https://doi.org/10.1039/C2DT30639E)
- 9 Wang, F.G.; Zhao, X.R.; Duan, L.B.; Wang, Y.J.; Niu H.R.; Ali, A.; *J. Alloy. Compd.*, **2015**, 623, 290.
DOI: [10.1016/j.jallcom.2014.10.117](https://doi.org/10.1016/j.jallcom.2014.10.117)
- 10 Pronina, N.; Klauson, D.; Deubener, J.; Knichevskaya, M.; *Appl. Cata. B. Env.*, **2014**, 178, 117.
DOI: [10.1016/j.apcatb.2014.10.006](https://doi.org/10.1016/j.apcatb.2014.10.006)
- 11 Abed, C.; Bouzidi, C.; Elhouichet, H.; Gelloz, B.; Ferid, M.; *Appl. Surf. Sci.*, **2015**, 349, 855.
DOI: [10.1016/j.apsusc.2015.05.078](https://doi.org/10.1016/j.apsusc.2015.05.078)
- 12 Wu, Y.; Yun, J.; Wang, L.Q.; Yang, X.; *Cryst. Res. Technol.*, **2013**, 48, 145.
DOI: [10.1002/crat.201200438](https://doi.org/10.1002/crat.201200438)
- 13 Barakat, N.A.M.; Taha, A.; Motlak, M.; Nassar, M.M.; Mahmoud, M.S.; Al-Deyab, S.S.; El-Newehy, M.; Kim, H.Y.; *Appl. Cata. A. Gen.*, **2014**, 481, 19.
DOI: [10.1016/j.apcata.2014.04.045](https://doi.org/10.1016/j.apcata.2014.04.045)
- 14 Long, M.; Cai, W.; Cai, J.; Zhou, B.; Chai, X.; *J. Phy. Chem.*, **2006**, 110, 20211.
DOI: [10.1021/jp063441z](https://doi.org/10.1021/jp063441z)
- 15 Zou, Z.G.; Ye, J.H.; Arakawa, H.; *Chem. Phy. Lett.*, **2000**, 332, 271.
DOI: [10.1016/S0009-2614\(00\)01265-3](https://doi.org/10.1016/S0009-2614(00)01265-3)
- 16 Klahr, B.; Gimenez, S.; Fabregatsantiago, F.; Bisquert, J.; Hamann, T.W.; *J. Am. Chem. Soc.*, **2012**, 134, 16693.
DOI: [10.1021/ja306427f](https://doi.org/10.1021/ja306427f)
- 17 Wu, Y.; Xia, C.; Zhang, W.; Yang, X.; Bao, Z.Y.; Li, J.; Zhu, B.; *Adv. Func. Mat.*, **2016**, 26, 938.
DOI: [10.1002/adfm.201503756](https://doi.org/10.1002/adfm.201503756)
- 18 Barakat, N. A. M.; Taha, A.; Motlak, M.; Nassar, M. M.; Mahmoud, M. S.; Al-Deyab, S. S.; El-Newehy, M.; Kim, H. Y.; *Appl. Cata. A. Gen.*, **2014**, 481, 19-26.
DOI: [10.1016/j.apcata.2014.04.045](https://doi.org/10.1016/j.apcata.2014.04.045)
- 19 Cao, Z. Q.; Qin, M. L.; Jia, B. R.; Gu, Y. R.; Chen, P. Q.; Volinsky, A. A. Qu, X. H.; *Ceram. Int.*, **2015**, 41, 2806-2812.
DOI: [10.1016/j.ceramint.2014.10.100](https://doi.org/10.1016/j.ceramint.2014.10.100)
- 20 Xie, J.; Zhang, L.; Li, M. X.; Hao, Y. J.; Lian, Y. W.; Li, Z.; Wei, Y.; *Ceram. Int.*, **2015**, 41, 9420-9425.
DOI: [10.1016/j.ceramint.2015.03.320](https://doi.org/10.1016/j.ceramint.2015.03.320)
- 21 Ilican, S.; Caglar, M.; Caglar, Y.; *Appl. Surf. Sci.*, **2010**, 256, 7204.
DOI: [10.1016/j.apsusc.2010.05.052](https://doi.org/10.1016/j.apsusc.2010.05.052)
- 22 Sing, K.S.W.; Everett, D.H.; Haul, R.A.W.; Moscou, L.; Pierotti, R.A.; Rouquerol, J.; Siemieniewska, T.; *Pure&Appl. Chem.*, **1985**, 57, 603.
DOI: [10.1351/pac198557040603](https://doi.org/10.1351/pac198557040603)
- 23 Kruk, M.; Jaroniec, M.; *Chem. Mater.*, **2001**, 13, 3169.
DOI: [10.1021/cm0101069](https://doi.org/10.1021/cm0101069)
- 24 Shukla, S.K.; Vamakshi; Minakshi; Bharadavaja, A.; Shekhar, A.; Tiwari, A.; *Adv. Mat. Lett.*, **2012**, 3(5), 421.
DOI: 10.5185/amlett.2012.5349
- 25 Hao, R.R.; Wang, G.H.; Tang, H.; Sun, L.; Xu, C.; Han, Y.D.; *Appl. Catal. B. Env.*, **2016**, 187, 47.
DOI: [10.1016/j.apcatb.2016.01.026](https://doi.org/10.1016/j.apcatb.2016.01.026)
- 26 Feng, X.H.; Guo, H.J.; Patel, K.; Hong, Z.; Xia, L.; *Chem. Eng. J.*, **2014**, 244, 327.
DOI: [10.1016/j.cej.2014.01.075](https://doi.org/10.1016/j.cej.2014.01.075)
- 27 Araújo, T.C.; Oliveira, H.D.S.; Teles, J.J.S.; Fabris, J.D.; Oliveira, L.C.A.; *Appl. Catal. B. Env.*, **2015**, 182, 204.
DOI: [10.1016/j.apcatb.2015.09.036](https://doi.org/10.1016/j.apcatb.2015.09.036)



A Monthly Journal

Publish your article in this journal

Advanced Materials Letters is an official international journal of International Association of Advanced Materials (IAAM, www.iaamonline.org) published monthly by VBRI Press AB from Sweden. The journal is intended to provide high-quality peer-review articles in the fascinating field of materials science and technology particularly in the area of structure, synthesis and processing, characterisation, advanced-state properties and applications of materials. All published articles are indexed in various databases and are available download for free. The manuscript management system is completely electronic and has fast and fair peer-review process. The journal includes review article, research article, notes, letter to editor and short communications.

Copyright © 2017 VBRI Press AB, Sweden www.vbripress.com/aml